Monitoring Tire-Road Friction Using The Wheel Slip

Fredrik Gustafsson

Tire-road friction estimation (TRFE) has become an intense research area as the interest of information technology in vehicles increases. For instance, the need of TRFE is established as the problem area "Common European Demonstrator 2.1," Friction Monitoring and Vehicle Dynamics, in the European Prometheus project and it is also identified by the Advanced Vehicle Control Systems Committee of the Intelligent Vehicle Highway Society of America [1]. TRFE is of importance in itself as a driver information unit, but friction information is also needed in other functions such as anti-locking brake systems (ABS), traction control, safety margin determination, autonomous intelligent cruise control, collision avoidance systems, and for exchange of road-side information.

In this work, we follow a model-based approach where the difference in wheel velocities of driven and non-driven wheels is used, as suggested in [2] and [3]. The perhaps most important feature is that only existing sensors are needed if the car is supplied with ABS brakes. The goal is to compute certain parameters from available standard sensors in the car, which depend directly or indirectly on the friction, and to find rules regarding how to evaluate the maximal friction forces that can be used for braking or cornering.

There are two problems of theoretical interest in this approach:

- Design an adaptive parameter estimator suitable for this application. It must give accurate estimates and at the same time be able to track fast variations.
- Determine the physical relation between these parameters and the maximal friction forces.

Here, we will concentrate on the first problem. However, most of the work in this project concerns the second problem, and results on this are reported in [3].

The order of presentation follows the signal flow in Figure 1. First, we give an overview and physical background, introduce notation and provide some results from test drives. A Kalman filter is applied to quantities computed from measurements (its design, giving the required accuracy, is described in the next section). Then four different change detectors to support the Kalman filter after abrupt changes are examined. Several different criteria for fault detection and surveillance are compared using Monte Carlo simulations. One section describes the change detector that has been implemented in a Volvo 850 and tested on public roads and test tracks for one year.

Background

Basic Definitions

The basic idea is to study the friction dependency in the so-called *slip*. The slip is defined as the relative difference of a driven wheel's circumferential velocity, $\omega_w r_w$, and its absolute velocity, v_w:

$$s = \frac{\omega r_w - v_w}{v_w}, \tag{1}$$

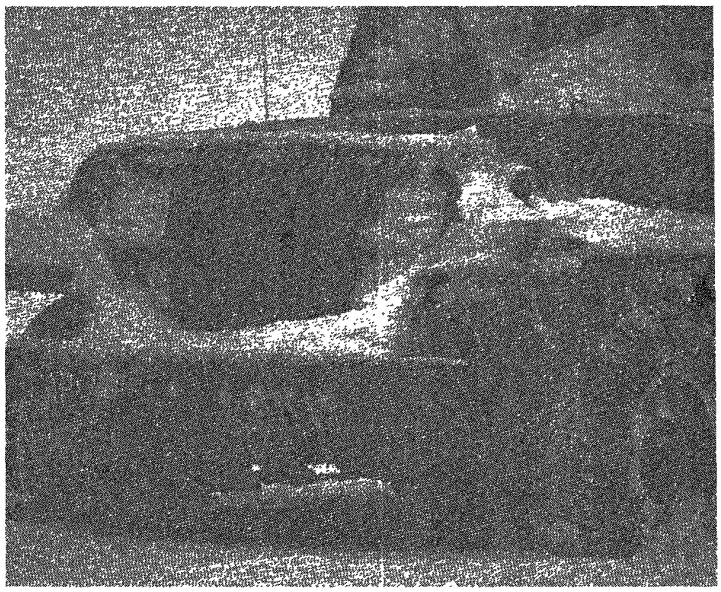

©Chris Hackett/The Image Bank

where r_w is the wheel radius. The absolute velocity of a driven wheel is computed from the velocities of the two non-driven wheels, assuming two-wheel drive, and geometrical relations in a straightforward manner. A convenient unit for slip is parts of a thousand.

We also define the *normalized traction force*, μ, (sometimes referred to as the friction coefficient) as the ratio of normalized traction force (F_f) and normal force (N) on one driven wheel,

$$\mu = \frac{F_f}{N}. \tag{2}$$

The author is with the Department of Electrical Engineering, Linköping University, SE-581 83 Linköping, Sweden, fredrik@isy.liu.se. *This is an extended version of a contribution to the 1996 IEEE Symposium on Computer Aided Control System Design. This work is a part of the project Driver Assistance and Local Traffic Management in the Swedish RTI program. Main sponsors are The Swedish Board for Industrial and Technical Development, AB Volvo, Saab-Scania AB and The Swedish National Road Administration.*

 0272-1708/98/$10.00©1998IEEE

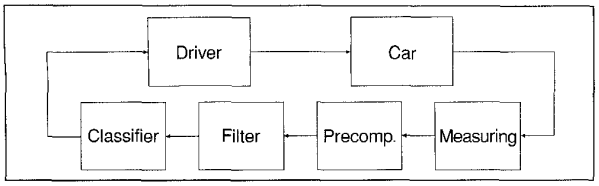

Fig. 1. Signal flow.

Also μ is computed from measurements, in this case a fuel injection signal, via an engine model. However, in the sequel we will consider s and μ as measurements.

Friction Model

A plot of the normalized traction force versus the slip, $\mu = \mu(s)$, shows a very significant characteristic which depends on the combination of tire and road. Figure 2 shows examples of test drives on asphalt and ice, respectively. The purpose of the filter is to adaptively estimate the straight line in Figure 2. Note the fundamental importance of *excitation*. There is no way to estimate both the slope and intersection of this line from constant values of the slip and normalized traction force, a fact that will be mathematically formulated below.

A careful examination shows that the slope is different for asphalt and ice, although the difference in slope can be as small as in the figure, so we define

$$k = \left.\frac{d\mu}{ds}\right|_{\mu=0} . \tag{3}$$

This slope k is commonly referred to as the *longitudinal stiffness* since it can be justified theoretically from the tire characteristics alone. A stiff tire gives a large k. According to classical presentations on tire models (see, for instance, Figure 1.16 in [4]), the slip slope depends solely on the tire until tire sliding occurs, which starts at approximately $s = 0.05$. Since this theory does not explain the friction dependency we have found in this project for slip measurements $s < 0.01$ that are available during normal driving, we prefer to call it simply the *slip slope*.

The basic assumption is that *the slip slope contains sufficient information to provide an accurate value of the friction.* The slip slope is estimated from the straight line assumption $\mu = ks$ for small slip values. It should be pointed out that this assumption is valid during normal driving, but not for large slip values. The assumption and classical theory give slip curves as sketched in Figure 3.

As seen from Figure 2, it is important to include an offset in the model,

$$\delta = s|_{\mu=0} . \tag{4}$$

That is, the slip is not zero when the normalized traction force is zero. This is partly due to rolling resistance and partly due to a small difference in wheel radii. Since the effective tire radius depends on wheel load, velocity and so on, δ will be time-varying. This offset must be compensated for when the slip slope is estimated.

Friction Classification

It turns out that the slip slope can take on almost any value on gravel roads. That is, gravel roads must be detected by other means. The proposed solution is to utilize the very coarse surface texture on gravel roads. The surface's coarseness gives a random contribution to the measurement of the angular velocity,

$$\omega = v / r_w + e.$$

Here v is the wheel's absolute velocity and v/r_w is the angular velocity one would get on a perfectly even surface. Now, we can define

$$\gamma = \mathrm{Var}(e)$$

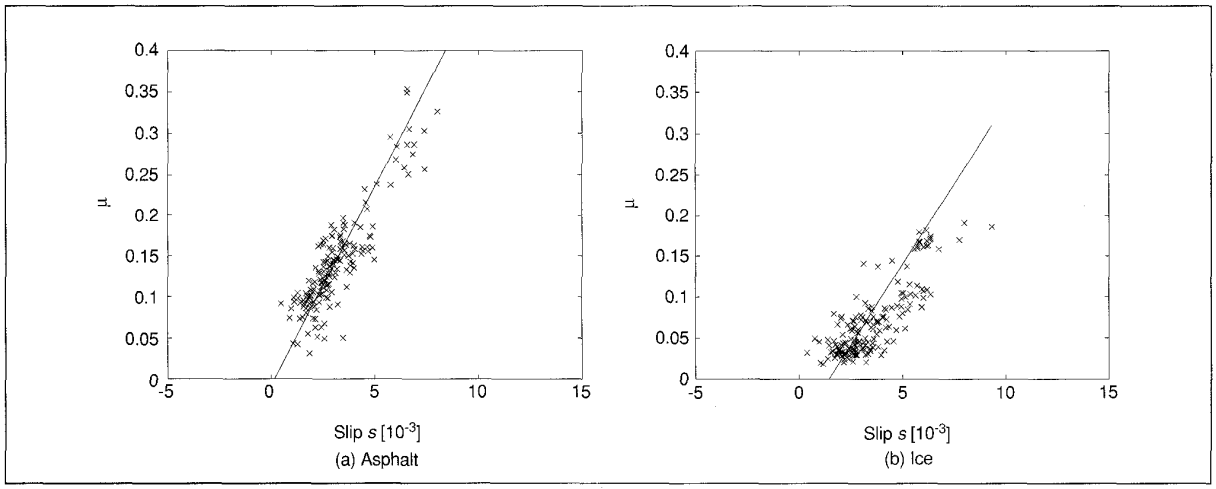

Fig. 2. Measurements of normalized traction force μ *and wheel slip* s *on dry asphalt (a) and hard snow (b), respectively. Circles denote measurements and the solid line is a straight line approximation obtained from the filter described in the section entitled "Filtering." Note the difference in slope (and also in offset).*

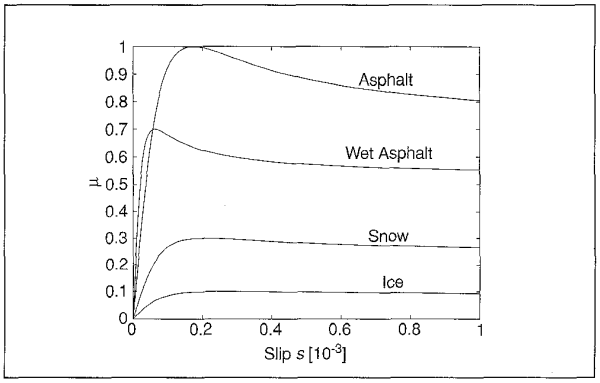

Fig. 3. Schematic plots of μ–s curves for different surfaces. The difference in initial slope for different friction conditions is exaggerated.

and use an estimate of it for detecting gravel.

To conclude this discussion, we have three quantities which depend on the friction: k, δ, γ. A number of test drives on surfaces with known properties can be illustrated as points in the space (k, δ, γ). To each point we hang a surface label, and if the approach is successful the labels from the same surface will cluster together. It turns out that the offset δ is not correlated with friction, and can be considered as nuisance. Omitting the offset δ, we get, for a particular tire, the plot in Figure 4.

It is clear from the figure that we can construct a classifier which works for this car and these tires and at this time. For instance, the following classifier can be used:

Gravel ($\mu \approx 0.5$) if $\gamma > 0.027$.
Asphalt ($\mu > 0.8$) if $\gamma < 0.027$ and $k > 30$.
Snow or ice ($\mu < 0.3$) if $\gamma < 0.027$ and $k < 30$.

As indicated above, it is not at all certain that this classifier works half a year later, or with different tires, or even on another car. This implies that the classifier has to be adaptive, which is a major problem. However, relative changes can still be detected. For a thorough discussion of these issues, see [3].

Alternative Approaches

Several different approaches to TRFE have been tried. Most of these are based on additional sensors. Acoustic and optical sensors, together with pattern recognition methods, is one possibility, and strain sensors in the tire is another. See [5] for an overview of these approaches. The use of acoustic sensors in combination with a neural net has been examined in [6]. A natural approach is to study the dynamical behavior of the car, such as using information from an active ABS system [7]. The drawback here is the requirement of much excitation, which is hardly the case during normal driving.

Filtering

Both s and μ are computed, without filtering, from measured quantities. An index m will be used to distinguish the measured quantities from the true ones. This section describes a linear filter to estimate the friction related parameters.

A Linear Regression Model

The goal is to derive a linear regression model, *i.e.* a model linear in the parameters, for which there exists efficient estimation methods. The slip slope k we want to compute is defined in (3) which for small μ reads (using (4))

$$\mu = k(s - \delta) \tag{5}$$

where also δ is unknown. Although this is a model linear in the parameters, there are two good reasons for rewriting it as

$$s = \mu \frac{1}{k} + \delta. \tag{6}$$

That is, we consider s to be a function of μ rather than the other way around, because s_m contains more noise than μ_m, and the parameter δ is varying much more slowly, compared to $k\delta$. Both these arguments facilitate a successful filter design. Note that all quantities in the basic equation (6) are *dimensionless*.

We will apply a filter where $1/k$ and δ are estimated simultaneously. The design goals are to

- get accurate values of k, while keeping the possibility of tracking slow variations in both k and δ and at the same time
- detect abrupt changes in k rapidly.

This will be solved by a Kalman filter, described in this section, supplemented by a failure detection algorithm detailed in the section "Real-Time Implementation."

The Kalman filter

We will now allow time variability in the parameters, $k(t)$ and $\delta(t)$. Basically, there are three methods to estimate time-varying parameters in a linear regression, namely Least Mean Square (LMS), Recursive Least Squares (RLS) with forgetting factor, and the Kalman filter. The first is much too slow for this application. The second has just one degree of freedom to adjust the

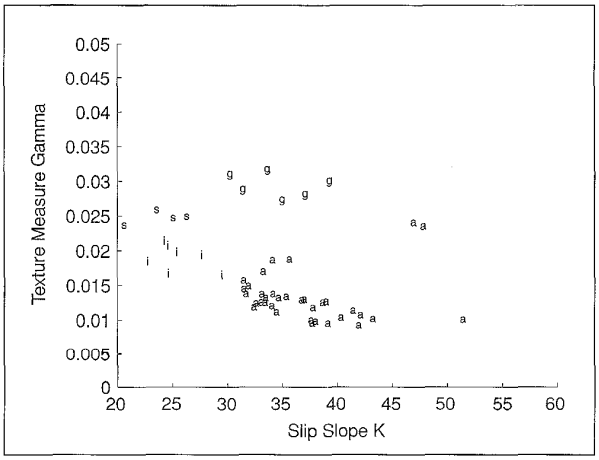

Fig. 4. Slip slope and a texture measure estimated for an M+S tire from field tests consisting of approximately 1000 measurements each. Each letter represents one field test and the abbreviations are: asphalt (a), gravel (g), snow (s) and ice (i). Note how test trials from the same surface cluster together, making friction classification possible.

adaptivity. We propose to use the Kalman filter because it is easily tuned to track parameters with different speeds.

Equation (6) is extended to a state space model where the parameter values vary like a random walk

$$\begin{aligned} \theta(t+1) &= \theta(t) + v(t) \\ y(t) &= \varphi^T(t)\theta(t) + e(t) \end{aligned}, \tag{7}$$

where

$$\begin{aligned} Q(t) &= \mathrm{E}v(t)v^T(t) \\ R(t) &= \mathrm{E}e(t)e^T(t) \\ y(t) &= s_m(t) \\ \varphi(t) &= (\mu_m(t), 1)^T \\ \theta(t) &= \left(\frac{1}{k(t)}, \delta(t)\right)^T. \end{aligned}$$

Here $v(t)$ and $e(t)$ are considered as independent white noise processes. Now the Kalman filter (see [8]) gives the optimal (in the minimum variance sense) parameter estimates $\hat{\theta}(t)$:

$$\begin{aligned} S(t) &= P(t-1) + Q(t) \\ K(t) &= S(t)\varphi(t)\left(\varphi^T(t)S(t)\varphi(t) + R(t)\right)^{-1} \\ \hat{\theta}(t) &= \hat{\theta}(t-1) + K(t)\left(y(t) - \varphi^T(t)\hat{\theta}(t-1)\right) \\ P(t) &= S(t) - K(t)\varphi^T(t)S(t). \end{aligned} \tag{8}$$

$P(t)$ is interpreted as the covariance matrix of the parameter estimates. The point with using the Kalman filter is that, assuming a diagonal structure of Q, the diagonal elements of Q are directly proportional to the tracking ability of the corresponding parameter.

Excitation Aspects

A well-known problem in the least squares theory occurs in the case of errors in the regression vector. A general treatment on this matter, usually referred to as *errors in variables* or the *total least squares* problem, is given in [9]. In our case, we have measurement and computation errors in the normalized traction force $\mu(t)$. Assume that

$$\mu_m(t) = \mu(t) + v_\mu(t), \quad \mathrm{Var}(v_\mu(t)) = \lambda_\mu \tag{9}$$

is used in $\varphi(t)$. Here $\mathrm{Var}(v_\mu(t))$ indicates the variance of the error in the measurement $\mu_m(t)$. Some straightforward calculations show that the noise in $\mu_m(t)$ leads to a positive bias in the slip slope,

$$\hat{k} \approx k\,\frac{\overline{\mathrm{Var}}(\mu) + \lambda_\mu}{\overline{\mathrm{Var}}(\mu)} > k. \tag{10}$$

Here $\overline{\mathrm{Var}}(\mu)$ is the variation of the normalized traction force defined as

$$\overline{\mathrm{Var}}(\mu) = \frac{1}{N}\sum_{t=1}^{N}\mu(t)^2 - \left(\frac{1}{N}\sum_{t=1}^{N}\mu(t)\right)^2. \tag{11}$$

This variation is identical to how one estimates the variance of a stochastic variable. Normally, the bias is small because $\overline{\mathrm{Var}}(\mu) \gg \lambda_\mu$. That is, the variation in normalized traction force is much larger than its measurement error.

The variation in normalized traction force also determines the stochastic uncertainty in the estimates, as shown by the following result for the parameter covariance $P(N) = \mathrm{Cov}\,\hat{\theta}(N)$ from N data assuming constant parameters and no adaptation ($Q = 0$):

$$\frac{1}{\det(P(N))} \sim \det\left(\sum_{t=1}^{N}\varphi(t)\varphi^T(t)\right) = N^2\,\overline{\mathrm{Var}}(\mu(t)). \tag{12}$$

That is, if the variation in normalized traction force is small during the time constant N of the filter, the parameter uncertainty will be large.

Experience From Test Trials

This section summarizes results in [3]. The filter has been running for more than 10000 km, and almost 1000 documented tests have been stored. The overall result is that the linear regression model and Kalman filter are fully validated. The noise $e(t)$ in (7) has been analyzed by studying the residuals from the filter, and can be well approximated by white Gaussian noise with variance 10^{-7}. The offset δ is slowly time varying and (almost) independent of the surface. Typical values of the slip slope k are also known, and, most importantly, they are found to differ for different surfaces. The theoretical result that filter performance depends on excitation in $\mu(t)$ is also validated, and it has also turned out that measurements for small slip and μ (i.e., $\mu(t) < 0.05$) values are not reliable and should be discarded.

A Comparison of Change Detectors

To overcome the drawback of slow tracking using linear filters (to be illustrated in the third sub-section below), we next compare some possible change detection methods. First, the simulation setup used throughout this section is described.

Simulation setup

The general knowledge summarized in the discussion of the test trials above makes it possible to perform realistic Monte Carlo simulations for studying the filter response, which is very hard to do for real data. What is important here is to use real measured $\mu(t)$, below denoted $\mu_m(t)$. The slip data is simulated from the slip model:

$$s(t) = 1/k(t)\mu_m(t) + \delta(t) + e(t). \tag{13}$$

The noise $e(t)$ is simulated according to a distribution estimated from field tests, while real data are used in $\mu_m(t)$. In the simulation,

$$\begin{aligned} \delta(t) &= 0.005, \quad k(t) = 40, \quad t < 200 \\ \delta(t) &= 0.005, \quad k(t) = 30, \quad t \geq 200 \end{aligned}$$

According to Figure 4, this corresponds to a change from asphalt to snow for a particular tire. The slip offset is given a high but still normal value. The noise has variance 10^{-7}, which implies that the signal is of the order 8 times larger than the noise. The specific normalized traction force $\mu(t)$ and one realization of $s(t)$ are shown in Figure 5.

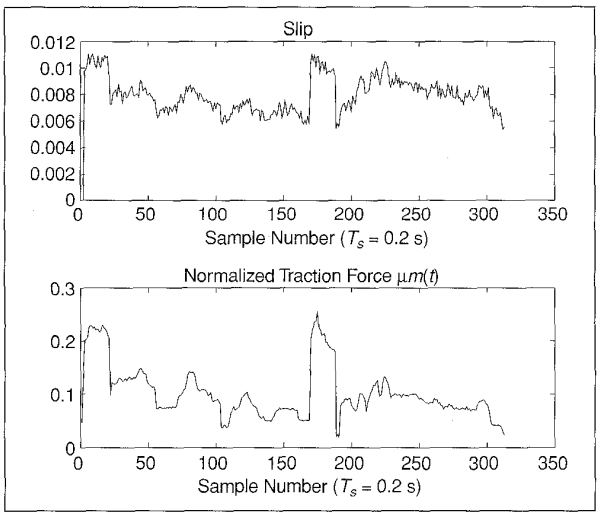

Fig. 5. The measured normalized traction force $\mu_m(t)$ (lower plot) and one realization of a simulated $s(t)$ (upper plot).

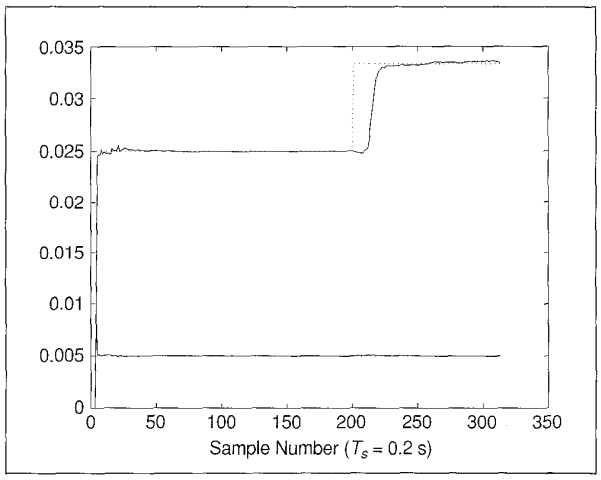

Fig. 6. Illustration of parameter tracking after an abrupt friction change at sample 200 using the data in Fig. 5 and a Kalman filter. The estimate is averaged over 100 realizations of $e(t)$ in (13).

As in the real-time implementation, the sampling interval 0.2 s is chosen. (Since there are no dynamics in the model, we feel the appropriate scale on the time axis in the figures is that given in the sample number.)

Note that the change time at 200 is carefully chosen to give the worst possible condition in terms of excitation, since the variation in normalized traction force is very small after this time (see the subsection "Excitation Aspects").

Computer Aid

The results presented herein are obtained using a general purpose Matlab toolbox for change detection. This toolbox has greatly decreased development time in this project. In fact, all of the results, figures, and the table, in this comparative study can be reproduced by a few mouse clicks.

A Linear Filter

First, the response of the Kalman filter presented in the previous section is examined. The design parameters are chosen as

$$Q(t) = \begin{pmatrix} 0.3 & 0 \\ 0 & 0 \end{pmatrix}.$$
$$R(t) = 1$$

This implies that the slip slope is estimated adaptively, while the offset has no adaptation mechanism. In practice, the (2,2) element of Q is assigned a small value. The result from the filter using the data in Figure 5 is shown in Figure 6.

It is evident that the convergence time of 50 samples, corresponding to 10 seconds, is too long.

Comparison of Change Detectors

The different methods in this section are designed to give a very low false alarm rate, while the remaining degrees of freedom are used to minimize the delay for detection. The tuning is done manually. A brief description of the methods is found below; see the references for a more detailed presentation.

- An RLS filter without forgetting, where the residuals are fed into a two-sided CUSUM detector (see [10] and the discussion of the CUSUM Test below), and the RLS filter is restarted after an alarm. The design parameters in the CUSUM test are a threshold $h = 3 \cdot 10^{-3}$ and a drift $\nu = 5 \cdot 10^{-4}$. The drift parameter effectively makes changes smaller than 5% impossible to detect. After a detected change, the RLS filter is restarted.
- The divergence test (DT) (see [11]). The design parameters are a sliding window length $M = 10$, a threshold $h = 10^{-6}$, and a drift $\nu = 5 \cdot 10^{-7}$.
- The Generalized Likelihood Ratio (GLR) test (see [12] and [11] and [13] as well). The GLR is the ratio of the likelihoods for no jump versus a jump at time k, maximized over the unknown parameters after the change. To get a feasible and recursive implementation, only jumps in the last 10 time instants are considered. In addition to the size of the sliding window (10), the design parameter is a threshold chosen as $h = 10^{-6}$.
- A bank of parallel RLS filters, each one matched to a certain hypothesis about the history of change times, and the maximum *a posteriori* (MAP) estimate is computed recursively. See [14] for details. This segmentation algorithm will be referred to as SEGM. The advantage of this method is that it contains no data dependent design parameters, so the default ones suggested in [14] are used. This is of course a great advantage in applications.

There are different ways to compare the examined methods. We have compared the following ones, among the first three ones are classical in-fault detection theory, and the next three are relevant in surveillance applications.

- Delay for detection (DFD).
- Missed detection rate (MDR).
- Mean time to detection (MTD).
- The sum of squared prediction errors from each filter,

$$V_N = \frac{1}{N} \sum_{0.1N}^{N} (y(t) - \varphi^T(t)\hat{\theta}(t))^2 .$$

- As argued in [15], the Minimum Description Length (MDL) can be interpreted as a norm for each method.
- The root mean square parameter error

$$PE = \frac{1}{N}\sum_{0.1N}^{N} \|\theta_0(t) - \hat{\theta}(t)\|^2 .$$

- Algorithmic simplicity, short computation time and design complexity. This kind of algorithm is implemented in C or even assembler, and the hardware is shared with other functionalities. There should be no design parameters if the algorithm has to be redesigned, for instance for another car model.

The parameter norm PE is perhaps a naive alternative, since the size of the parameter errors is not always a good measure of performance. Nevertheless, it is a measure of discrepancy in the parameter plots to follow.

Figures 7 and 8 show the parameter estimate from these filters averaged over 100 realizations and the alarm times histogram, respectively. The main problem with the CUSUM test is the transient behavior after an alarm. In this implementation, a new identification is initiated after each alarm, but there might be other (non-recursive) alternatives that are better. The divergence test is applicable, though not intended for general linear regression models, so here its performance is poor with large variation between the realizations. GLR and SEGM perform very well, both in terms of fast alarms and good parameter tracking.

The quantitative results are summarized in Table 1. The forgetting factor in RLS is optimized to minimize the loss function V_N. The other parameters are chosen to give zero false alarm rate and the best possible performance. There is no clear winner. In terms of performance and design simplicity, the SEGM function has a clear edge, even when considering a slightly longer delay for detection compared to GLR. Of crucial importance is the lack of design parameters in SEGM, which can be interpreted as a built-in robustness. Taking computation time and algorithmic complexity into account, the CUSUM test is a good alternative despite the delay for detection being twice as large.

Here it should be remarked that the design parameters in CUSUM, DT and GLR are hand-tuned, so their performances might be improved a little.

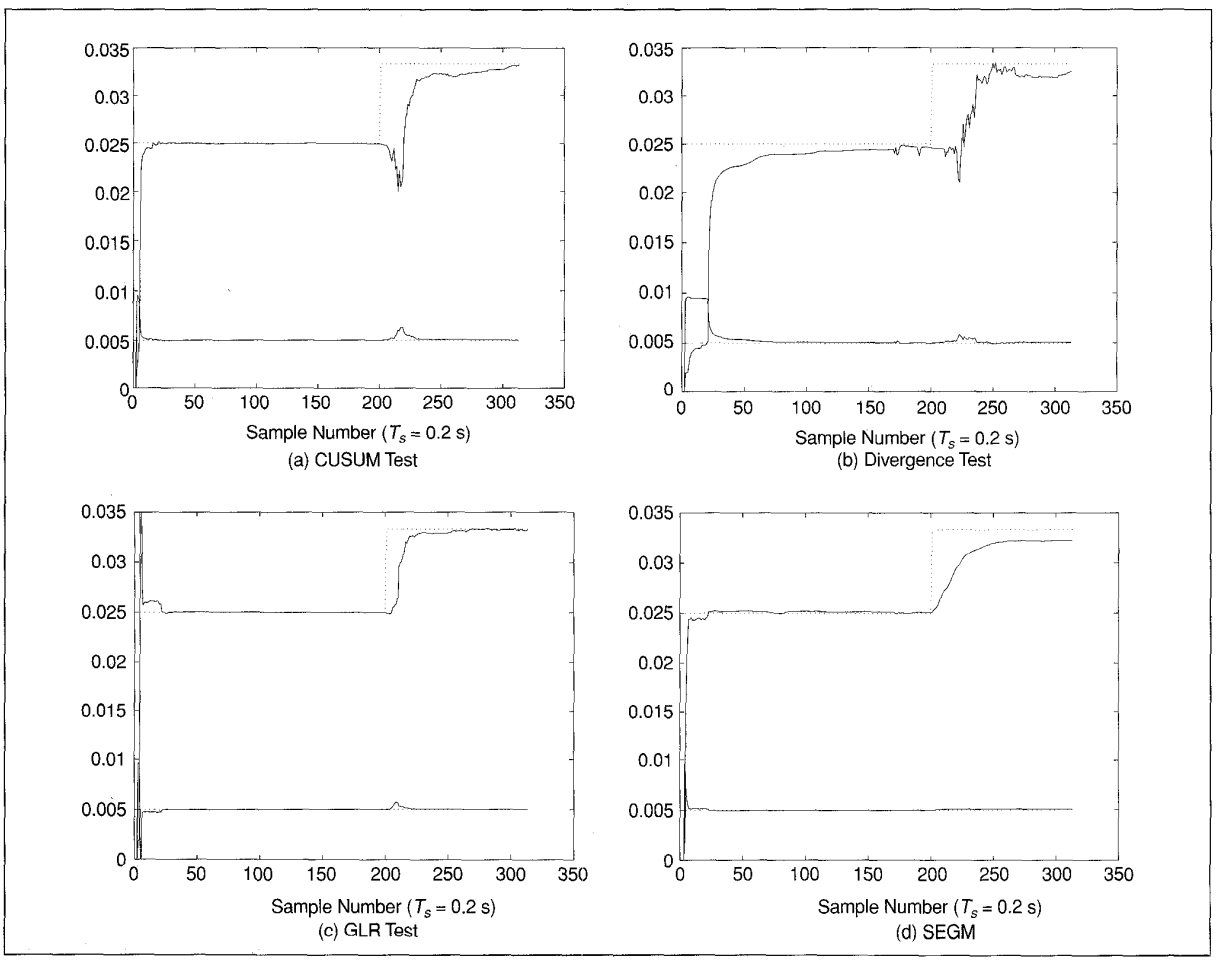

Fig. 7. Illustration of parameter tracking after an abrupt friction change at sample 200 using the data in Figure 5 and CUSUM (a), divergence test (b), GLR (c) and SEGM (d), respectively. The estimates are averaged over 100 realizations.

Real-Time Implementation

The design goals for the real-time application are as follows.

- It must be computationally fast.
- The mean time to detection should be on the order of a few seconds, while the mean time between false alarms should be quite large in the case where the driver is informed about the alarms. (If the system is only used for friction surveillance, the false alarm rate is not critical.)

The first condition rules out on-line versions of GLR and the SEGM algorithms at an early stage, although the hardware used in the current prototype would allow more computations. This would be a simple way to increase the performance. On the other hand, the CUSUM test satisfy both conditions. The next subsections describe the chosen algorithm.

The CUSUM Test

The tracking ability of the Kalman filter is proportional to the size of Q. The Kalman filter is required to give quite accurate values on the slip slope and has (by necessity, see [8]), a small Q. On the other hand, we want the filter to react quickly to sudden de-

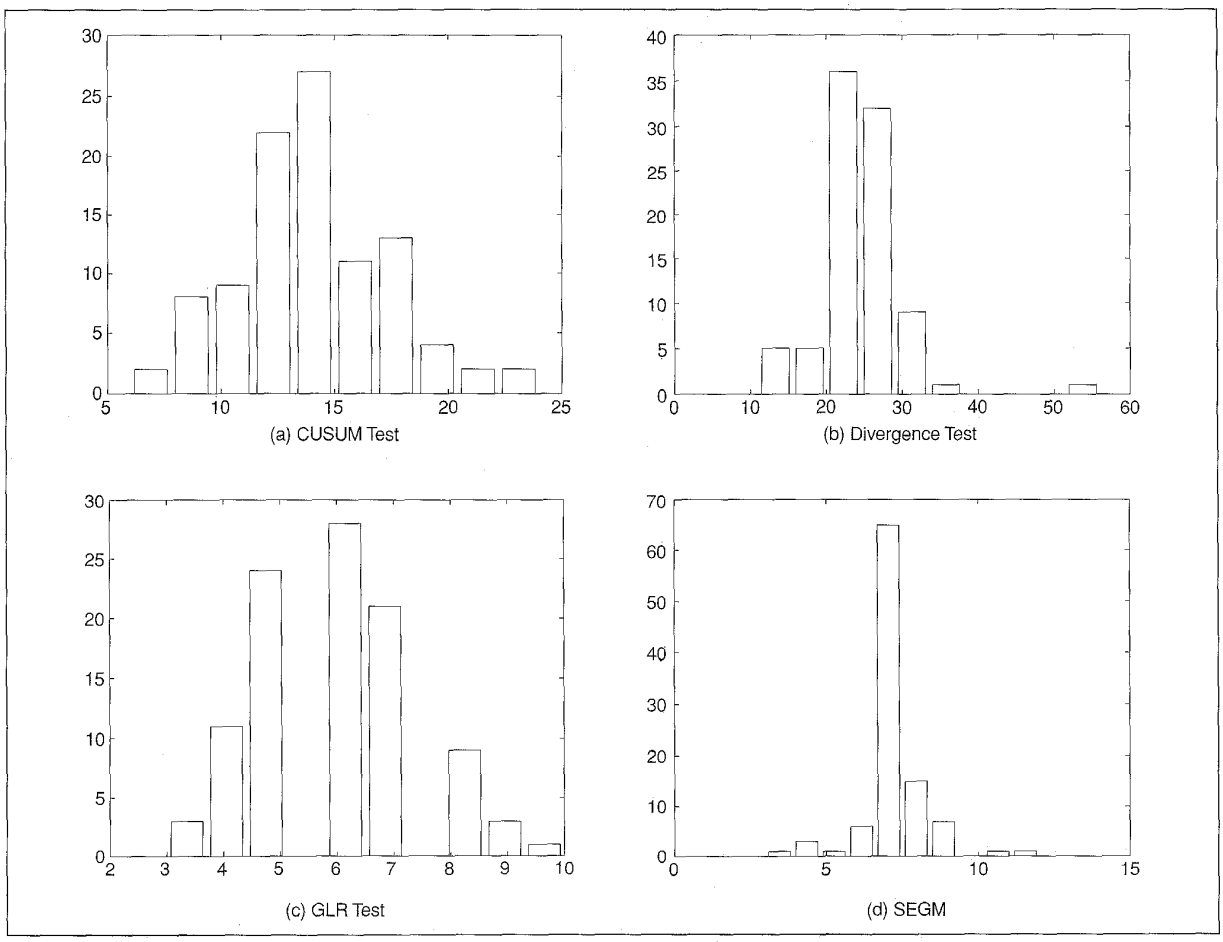

Fig. 8. Histogram over delay for detection in number of samples ($T_s = 0.2$ s) for CUSUM (a), divergence test (b), GLR (c) and SEGM (d) for 100 realizations.

Table 1. Comparison of some norms for the examined filters. The smaller the norm, the better the performance.

Method	MTD	MDR	FAR	V_N	MDL	PE	Time
RLS	—	—	—	$1.57 \cdot 10^{-7}$	$5.1 \cdot 10^{-7}$	0.0043	1
CUSUM	14.7	0	0	$1.41 \cdot 10^{-7}$	$6.3 \cdot 10^{-7}$	0.0058	1.11
DT	26	0	0.001	$1.86 \cdot 10^{-7}$	$8.9 \cdot 10^{-7}$	0.0100	1.58
GLR	5.9	0	0	$1.44 \cdot 10^{-7}$	$6.0 \cdot 10^{-7}$	0.00037	3.67
SEGM	7.1	0	0	$1.38 \cdot 10^{-7}$	$1.8 \cdot 10^{-7}$	0.00047	2.99

creases in k due to worsening friction conditions. This is solved by running the CUSUM detector in parallel with the Kalman filter. If it indicates that something has changed, then the diagonal elements of Q corresponding to the slip slope are momentarily increased to a large value. This allows a very quick parameter convergence (typically one or two samples).

In [11] a thorough treatment of the CUSUM test is given. In words, it looks at the prediction errors $\varepsilon_t = s_m(t) - \varphi^T(t)\hat{\theta}(t)$ of the slip value. If the slip slope has actually decreased, we will get predictions that tend to underestimate the real slip. The CUSUM test gives an alarm when the recent prediction errors have been sufficiently positive for a while. Mathematically, the test is formulated as the following time recursion:

$$\begin{aligned} g_0 &= 0 \\ g_t &= g_{t-1} + \varepsilon_t - \nu \\ g_t &= \max(g_t, 0) \\ \text{if } g_t &> h \text{ then alarm and } g_t = 0, \end{aligned} \tag{14}$$

where h is a threshold and ν a drift parameter.

The CUSUM test (14) gives an alarm only if the slip slope decreases. A similar test, where the sign of ε is changed, is used for detecting increases in slip slope. The combination of two such CUSUM detectors is referred to as a two-sided CUSUM test.

Example of Filter Response

In this section, an example is given to illustrate the interaction between the Kalman filter and the change detector, using data collected at the test track CERAM outside Paris. A road with a sudden change from asphalt to gravel and then back to asphalt is considered. Figure 9 shows the estimated slip slope as a function of time in one of the tests, where the gravel path starts after 8 seconds and ends after 16 seconds. Gravel roads have a much smaller slip slope than asphalt roads.

Note that the Kalman filter first starts to adapt to a smaller slip slope at $t = 8$ s, but after 3 samples (0.6 s) something happens. This is where the CUSUM detector signals for an alarm and we have convergence after one more sample. A similar behavior is noted at the end of the gravel path. The Kalman filter first increases k slightly; after some samples it speeds up dramatically, at which point it takes a couple of seconds to converge to a stable value.

Conclusions

We have described how a Kalman filter together with a CUSUM change detector has been implemented on a Volvo 850 GLT for real-time friction estimation. Since high accuracy is needed the Kalman filter must be tuned to be quite slow. Consequently, as both real data evaluation and simulation show, a change detector is needed to get fast tracking and to quickly alarm the driver for sudden changes in friction. The CUSUM detector was compared to some other change detectors; all of them satisfy the real-time requirements. The CUSUM test was chosen to be implemented and tested in real-time because of its simplicity and low complexity, although performance was slightly worse. Simulations as well as real data indicate good performance of the filter and detector, and the alarm time after a change is in the order of a second (five samples).

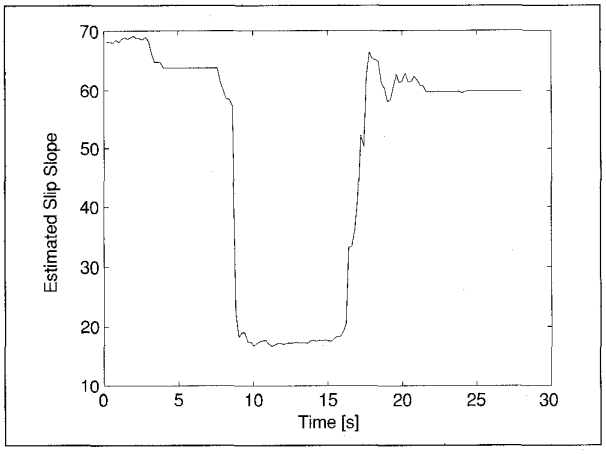

Fig. 9. Illustration of tracking ability in the estimated slip slope as a function of time. After 8 s an asphalt road changes to a short gravel path that ends at 16 s, so the true slip slope is expected to have abrupt changes at these time instants.

References

[1] S.E. Shladover, "Research and development needs for advanced vehicle control systems," *IEEE Micro*, pp. 11-19, February 1993.

[2] T. Dieckmann, "Assessment of road grip by way of measured wheel variables," *Proc. FISITA*, London, June 1992.

[3] F. Gustafsson, "Slip-based estimation of tire - road friction," *Automatica*, vol. 33, pp. 1087-1099, 1997.

[4] J.Y. Wong, *Theory of Ground Vehicles*. New York: John Wiley & Sons, 2nd ed., 1993.

[5] U. Eichhorn and J. Roth, "Prediction and monitoring of tyre/road friction," *Proc. FISITA*, London, June 1992.

[6] A. Svärdström, "Classification of road surface using a neural net (in Swedish)," Uppsala University, Uppsala, Sweden, Tech. Rep. UPTEC 93 056R, June 1993.

[7] U. Kiencke, "Realtime estimation of adhesion characteristic between tyres and road," *Proc. IFAC Congress*, pp. 15-18, Sydney, 1993.

[8] B.D.O. Anderson and J.B. Moore, *Optimal Filtering*, Prentice Hall, 1979.

[9] S. van Huffel and J. Vandewalle, "The total least squares problem," *SIAM*, Philadelphia, 1991.

[10] E.S. Page, "Continuous inspection schemes," *Biometrika*, vol. 41, pp. 100-115, 1954.

[11] M. Basseville and I.V. Nikiforov, *Detection of abrupt changes: theory and application*, Prentice Hall, 1993.

[12] A.S. Willsky and H.L. Jones, "A generalized likelihood ratio approach to the detection and estimation of jumps in linear systems," *IEEE Trans. Automatic Control*, vol. 21, pp. 108-112, 1976.

[13] F. Gustafsson, "The marginalized likelihood ratio test for detecting abrupt changes," *IEEE Trans. on Automatic Control*, vol. 41, pp. 66-78, 1996.

[14] Fredrik Gustafsson, *Estimation of discrete parameters in linear systems*, Dissertation no. 271, Linköping University, Sweden, 1992.

[15] F. Gustafsson, "A generalization of MDL for choosing adaptation mechanism and design parameters in identification," *SYSID'97*, Japan, vol. 2, pp. 487-492, 1997.

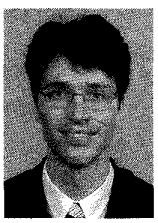

Fredrik Gustafsson was born in 1964. He received the M.S. degree in electrical engineering in 1988 and the Ph.D. degree in automatic control in 1992, both from Linköping University, Sweden. He is an associate professor in electrical engineering at Linköping University. His research is focused on statistical methods in system identification and signal processing, with applications to communication, avionic and automotive systems.